Characterization of Electron Deficient Oxide Ion of Heat Treated MgO for Activation of Methane

Takashi Karasuda and Ken-ichi Aika*

Department of Environmental Chemistry and Engineering, Interdisciplinary Graduate School of Science and Engineering, Tokyo Institute of Technology, 4259 Nagatsuta, Midori-ku, Yokohama 226-8502

(Received December 2, 1997)

Electron deficient oxide ions on the heat-treated MgO were characterized by temperature programmed desorption (TPD), X-ray photoelectron spectroscopy (XPS), and other methods (electron spin resonance (ESR) and Fourier transform infrared spectroscopy (FT-IR)). The O1s XP spectrum of MgO evacuated at 873 K has a very small shoulder peak (533.8 eV) at the higher binding energy (BE) side of the O^{2-} peak (at 531.5 eV). Upon the evacuation of 973 K, this shoulder peak increased remarkably, and at the same time H_2 started to be evolved (TPD). Since H_2 must be produced from a dissolved water in the bulk or surface OH without forming O_2, the surface oxygen must have a charge lower than 2. Thus, the shoulder peak was assigned to O^-. This state was not observable by ESR and not reactive to methane at room temperature (FT-IR), while O^- produced on the UV-irradiated MgO was ESR-observable and reactive. However, the heat-treated surface O^- must react with methane during the oxidative coupling of methane (OCM) reaction at 973 K. The two kinds of states for O^- on MgO are discussed from the standpoint of the defect chemistry.

Two kinds of catalysts, the redox type and the irreducible oxide type, are used for the oxidative coupling of methane (OCM) reaction. The first examples are PbO/Al_2O_3,[1] PbO/MgO,[2] and others, which give the low C_2 selectivity in the OCM reaction owing to the strong oxidation property. The second examples are Li/MgO,[3,4] Na/MgO,[5,6] and others, which give the high C_2 selectivity in the OCM reaction. An active site of the (irreducible) MgO-based catalysts for the OCM reaction has long been studied. The electron deficient oxide ions, which have lower electron charges than O^{2-} such as O^-, have been proposed to have an important role in the methane activation, which is to derive hydrogen from methane. Generally, the O^- production is accompanied with the formation of defects in the MgO lattice, for example, through doping with alkali metal ions[7] or by impurity water in the MgO lattice.[8] The O^- formation by Li^+ addition has been examined by electron spin resonance (ESR)[4] and the addition of Li^+ to MgO increased the C_2 selectivity on the OCM reaction. However, there has been no sufficient information yet about Li^+ free MgO. We have learned that H_2 desorption which originated from the dissolved water in MgO initiates the formation of the active oxygen species for the OCM reaction.[9—11] However, these species have not been confirmed by any spectroscopic methods.

In this research, we aimed to examine the MgO surface which was activated at high temperature so as to desorb H_2 by various methods such as X-ray photoelectron spectroscopy (XPS), Fourier transform infrared spectroscopy (FT-IR) and ESR and to compare those results with the activity of the OCM reaction; we build on the many pioneering works about the characterization of the MgO surface.[12,13]

Experimental

An MgO sample (purchased from Soekawa Chemicals, 99.96%) was treated with water, then dried and pressed.[10,11] For the temperature programmed desorption (TPD) experiments, the MgO sample was baked in air at 1273 K for 24 h. MgO samples for XPS and FT-IR measurements were used without baking in air at 1273 K. TPD runs were performed in a closed circulation system made of pyrex, which was almost the same as the system reported.[14] The residual pressure of the closed circulation system was below 10^{-6} Torr (1 Torr = 133.322 Pa). After being installed in a quartz reactor, the sample (0.2 g) was evacuated at 1173 K for 1 h (first heating) and cooled. Without further contact with H_2O, the TPD run was started from room temperature to 1173 K with a heating rate of 10 K min^{-1} (second heating). The desorption of H_2O, H_2, and O_2 from the MgO sample were analyzed by an on-line quadrupole mass spectrometer (NEVA NAG-515 MASS FILTER). The amount of desorption during the second heating (TPD) depended on the conditions (temperature and time) of the first heating.

For the XPS measurement, the dried MgO sample was ground and pressed under 200 kg cm^{-2} and crushed into 2-mm sized pellets. The samples were evacuated at the scheduled temperatures between 873—1173 K for 1 h (first heating) and cooled in vacuum. The samples were set on a standard sample holder of the instrument by a film of carbon-adhesive tape and transferred into the transfer-vessel of the XPS instrument VG ESCALAB 220i (Mg $K\alpha$ 400 W) under Ar atmosphere. The absolute values of the binding energy of each peak were calculated assuming the magnesium core level peak position: Mg2p as 50.8 eV.[15] XPS data was analyzed by using a PC program (Eclipse ver. 1.6 for OS/2).

Each MgO disk with a 10-mm diameter for the IR measurements was prepared by grinding 80 mg of MgO sample in an agate mortar and by pressing at 300 kg cm^{-2}. The IR cell was made of quartz, both sides of which were connected to aluminum flanges with an

epoxy-adhesive resin and the NaCl windows with Viton-O rings.[16] The cell equipped with Kanthal heating wire, Cu tube for water cooling, and SUS tube for liq. N_2 cooling. The IR cell is attached to the pyrex closed circulation system through two greaseless stopcocks. A JASCO FT/IR-350 with a resolution of 0.2 cm^{-1} was used. ESR measurements were carried out by JES-FE1X (JEOL) in a similar manner to that described elsewhere.[16]

Results

TPD. The TPD spectra of H_2O and H_2 from the MgO sample are shown in Fig. 1. It should be noted that the water desorption is rather small compared with the H_2 desorption. The data shown here are results of the second heating, where most of the water has been eliminated by the first heating (1173 K, 1 h). But still, water and H_2 were produced. As is seen from Fig. 1, H_2O desorption decreases above 1200 K, while H_2 (probably a decomposition product of H_2O) is desorbed even at high temperatures (above 1200 K). Another interesting point is that O_2 desorption can not occur up to 1273 K.

Surface Oxygen Species Observation by XPS. The O1s XP spectrum of MgO evacuated at 873 K is shown in Fig. 2(a). It has a very small shoulder peak at the higher BE side of the O^{2-} peak (at 531.5 eV). Upon the evacuation of 973 K, this shoulder peak increased gradually, as is shown in Fig. 2(b), and continued to increase as the evacuation temperature was raised. The deconvoluted top peak (533.6 eV) is positioned higher than the peak of either MgO (531.2 eV) or $Mg(OH)_2$ (532.5 eV), and is nearly at the same position as the shoulder peak of O1s of Li/MgO (533.6 eV). The C1s XP spectrum of MgO pretreated at 1073 K is shown in Fig. 2(d). It is composed of two peaks at 286.6 and 290.2 eV, which are shown in Fig. 2(d). The first peak at 286.6 eV was assigned to amorphous carbon in the chamber. The weak peak at 290.2 eV was assigned C1s of CO_3^{2-}.[17]

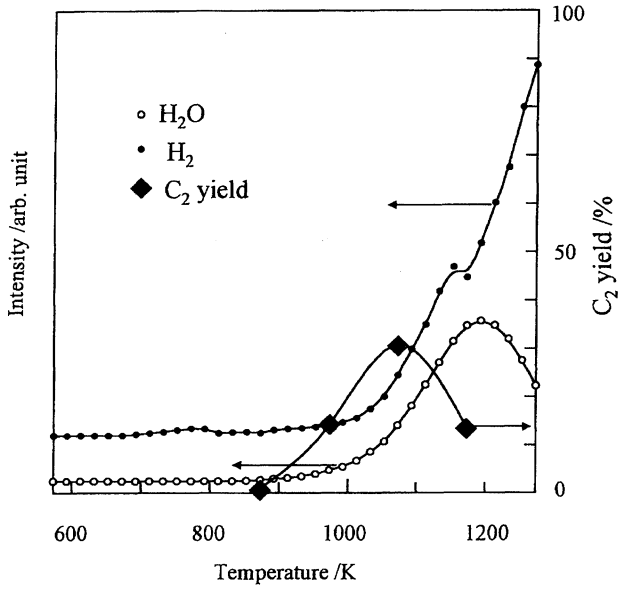

Fig. 1. TPD spectra of H_2O (open symbol) and H_2 (closed symbol) from MgO with a heating rate of 10 K min^{-1} and temperature dependence of C_2 yield on MgO.

Oxygen Species Observation by IR and ESR. After MgO is evacuated and UV-irradiated, N_2O introduction leads to the formation of O^-, which can be identified by ESR.[18] This species is reactive with CH_4 at room temperature. The resultant surface methoxide is observable with FT-IR on MgO, which is shown as a reference in Fig. 3(a). The peaks due to C–O bond of the methoxide are observed at 1053 and 1107 cm^{-1}.[16,19]

Similar experiments were done for the heat-treated MgO. No ESR peaks ascribable O^- or O_2^- were not observed

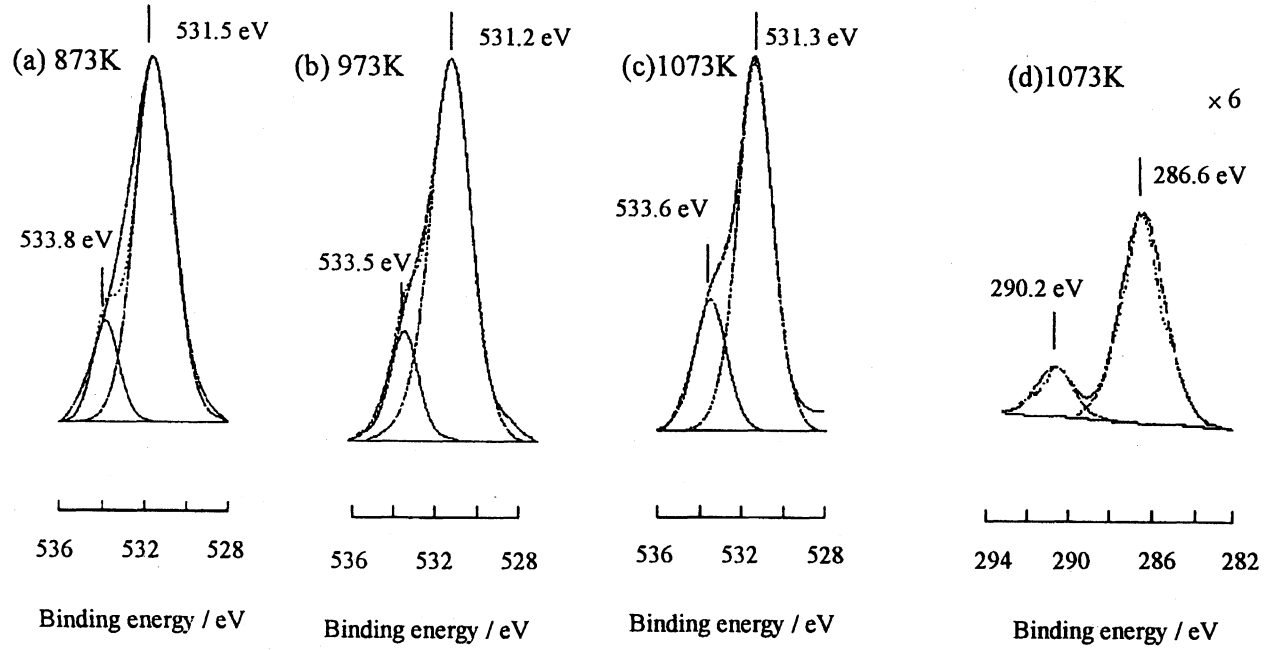

Fig. 2. The O1s XP spectra of MgO evacuated at 873 K (a) and 973 K (b), and 1073 K (c) respectively and the C1s XP spectra of MgO evacuated at 1073 K (d).

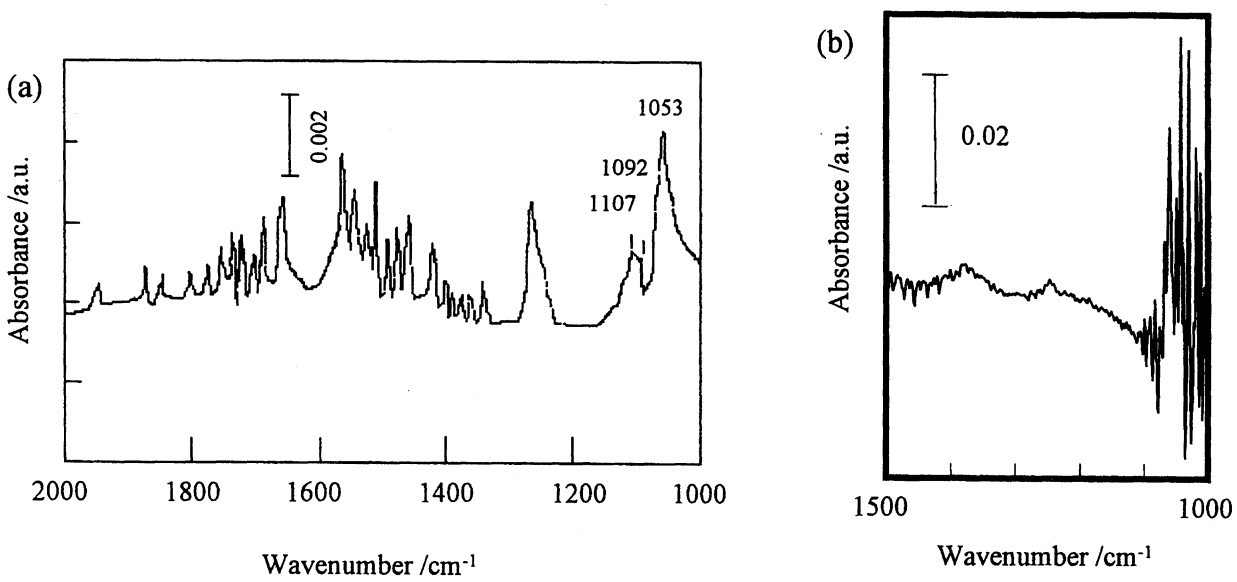

Fig. 3. FT-IR spectra of products of CH_4 on the UV-irradiated MgO (a) and the 1073 K-evacuated MgO at room temperature (b).

after heat treatment at 1073 K. The 1073 K evacuated MgO sample was also studied by spectroscopically FT-IR after CH_4 (25 Torr) was introduced and the sample was evacuated at room temperature. The spectrum is shown in Fig. 3(b), where no peak due to methoxide was not observed around 1100—1300 cm^{-1}. From these results, we concluded that the heat-treated MgO sample has not such species like the O^- on the UV-irradiated MgO and is inactive to CH_4 at room temperature (but active above 973 K).

Discussion

Electron Deficient Oxide Ion Formation through H_2 Desorption. MgO contains H_2O, a part of which enters into the MgO lattice and later becomes $Mg(OH)_2$ or surface hydroxides (Eq. 1). The desorbed H_2O is considered to come from the lattice water (Eq. 2) and hydroxyls (Eq. 3). Kroger–Vink terminology is also used.[20]

$$MgO + H_2O = MgO(H_2O) = Mg(OH)_2 \quad \text{i.e.} \quad Mg^X_{Mg}O^X_O(H_2)^X_{Mg}O^X_O \tag{1}$$

$$MgO(H_2O) \rightarrow MgO + H_2O\uparrow \quad \text{i.e.} \quad Mg^X_{Mg}O^X_O V''_{Mg}V^{\cdot\cdot}_O \tag{2}$$

$$Mg(OH)_2 \rightarrow MgO + H_2O\uparrow \quad \text{i.e.} \quad Mg^X_{Mg}O^X_O V''_{Mg}V^{\cdot\cdot}_O \tag{3}$$

$$Mg(OH)_2 \rightarrow MgO(O) + H_2\uparrow \quad \text{i.e.} \quad Mg^X_{Mg}O^X_O V''_{Mg}O^{\cdot\cdot}_O \tag{4}$$

$$MgO(O) = Mg^{2+} + O_2^{2-} = Mg^{2+} + 2O^- \quad \text{i.e.} \quad Mg^X_{Mg}O^{\cdot}_O V''_{Mg}V^{\cdot}_O \tag{5}$$

A part of hydroxyls are going to be decomposed to give H_2 (Eq. 4), as is shown in Fig. 1. It is to be noted that O_2, another decomposition product of H_2O, was not observed. The excess oxygen atoms are probably energetically high (reactive) and in a coordinatively unsaturated state (O_{CUS}: coordinatively unsaturated sites) with the lattice defects, because H_2 desorption leaves a vacancy, $O^{\cdot}_O V''_{Mg} O^{\cdot}_O$.[21] The O_{CUS} is thought to have an important role in the methane activation in the irreducible catalyst.[22] This O_{CUS} must be the electron deficient oxide ions, O^- (as is shown in Eq. 5), from the charge neutrality rule. Among the electron deficient oxide ions (O_2^-, O_2^{2-}, O^-, and O_3^-), the dissociated one (O^-) should be prevailing at high temperature. The O^- is assumed to be the active species for the OCM reaction. Indeed, C_2 yield of the OCM starts to increase at the temperature where H_2 desorption starts, as shown in Fig. 1, but the excess amount of O^- and high temperature result in the successive oxidation of methyl radicals, giving low C_2 yield. We tentatively refer to this as thermally generated O^- ($O^-(t)$).

Surface Oxygen Species Observation by XPS. O1s XP spectra of MgO evacuated at the high temperature have the shoulder peak at higher energy side. The position of this shoulder peak is consistent with that of the [Li^+O^-] peak. So this shoulder peak can be assigned to the electron deficient oxide ion which resembles [Li^+O^-], which is referred to as $O^-(t)$ here. Now, we suspect that the surface carbonate oxygen may contribute to the shoulder too. Because carbonate oxygen is said to give a similar binding energy (533.5 eV) to that of O^-.[15] If we look at the C1s XP spectra, our sample has CO_3^{2-} peak at 290.2 eV. Now the shoulder peak of O1s was found to be composed of $O^-(t)$ and the carbonate oxygen. In order to calculate the peak area of $O^-(t)$, the peak area of O1s of CO_3^{2-} was calculated from the C1s peak of CO_3^{2-} using the atomic sensitivity factors of the XPS[23] which Peng et al. calculated.[15] These results are shown in Table 1. The area of O^{2-} was also calibrated and compared with the Mg^{2+} area to check the accuracy of this method. The calculated atomic ratio of O^{2-} to Mg^{2+} was 1.0±0.1. This must support

Table 1. XPS Analysis of MgO Samples as a Function of the Evacuation Temperature

Evacuation	Shoulder peak of O1s		O1s of O^-		O1s of O^{2-}		C1s of CO_3^{2-}		O/Mg[d]
temperature/K	BE/eV	$(O^- + CO_3^{2-})$[a]	BE/eV	$r(O^-)$[b]	BE/eV	$r(O^{2-})$[b]	BE/eV	$r(CO_3^{2-})$[c]	
873	533.8	0.03	533.8	0	531.5	1.02	290.7	0.01	1.0
973	533.5	0.15	533.5	0.08	531.2	1.04	290.8	0.02	1.1
1073	533.6	0.18	533.6	0.12	531.3	0.88	290.6	0.02	1.0
1173	533.6	0.21	533.6	0.16	531.2	0.88	290.2	0.02	1.0

a) Atomic ratio of O (O^- and CO_3^{2-}) to Mg from the calibrated XPS area. b) Atomic ratio of O (O^- or O^{2-}) to Mg from the calibrated XPS area. c) Atomic ratio of O (originated to CO_3^{2-}) to Mg from the calibrated XPS area. d) Atomic ratio of O (originated to MgO) to Mg from the calibrated XPS area.

the other calculations such as the C to O ratio, although the XPS is a rather rough method for quantitative analysis.

The percentage of O1s shoulder peak and O^-(t) peak against the whole O1s of MgO is shown as a function of the evacuation temperature in Fig. 4. The O^-(t) generation is initiated at 973 K. These results roughly agreed with the results for Li–MgO and pure MgO in HREELS.[24—26] Wu et al. investigated $[Li^+O^-]$ production on Li/MgO by HREELS as the function of evacuation temperature. They reported the formation of not only $[Li^+O^-]$ but also F center. F centers are initiated at c.a. 1000 K on Li/MgO, and at c.a. 1100 K on pure MgO. Wu et al. have considered that F centers are generated on account of the multivalent transition metals as impurities, probably the distortion makes much $V_{Mg}^X V_O^X$ (V_O^X contains two electrons) at high temperature. But they did not take into account H_2O desorption, and H_2 desorption above 973 K as shown in our TPD results. The former may bring about their F center ($V_{Mg}^X V_O^X$), and the latter should bring about $V''_{Mg}+2O^\bullet_O$ (Mg^{2+} vacancy and two O^-) or p-type conduction. The OCM activity seems to be related with both F-center and O^- (p-type conduction), however, the accumulated results show that OCM is related with p-type conduction.[27] This temperature dependence of O^-(t) (Fig. 4) almost corresponds to that of H_2 desorption (Fig. 1).

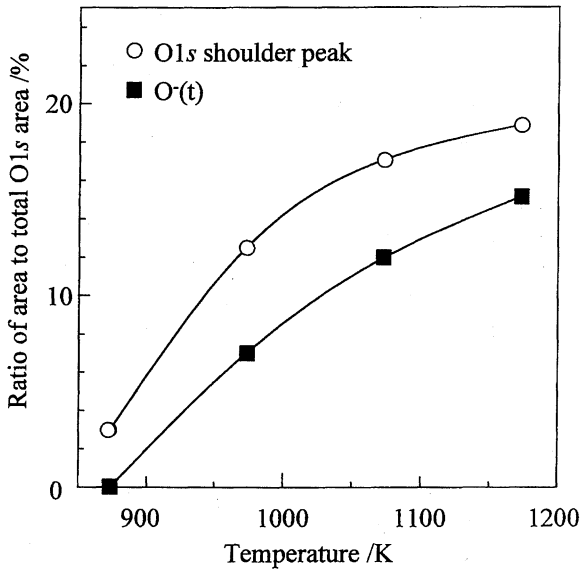

Fig. 4. Ratio of the O1s shoulder peak (○) and O^-(t) (■) to total O1s on MgO as a function of the evacuation temperature.

It is to be noted that the ratio of O^-(t) to the surface oxygen ion exceeds over 10% when evacuated at 1073 K. Similar XP spectra have already been recorded; however, the identification of O^- has not been done because the shoulder might be overlapped with a OH^- peak.[13]

Reactivity of the Electron Deficient Oxide Ion Generated by the High Temperature Treatment. Many scholars have reported the electron deficient oxide ion observed by XPS. Inoue et al. have observed the electron deficient oxide ion (O^-), which was positioned at the higher energy side than O^{2-} peak on alkali earth metal oxides such as CaO and BaO by XPS when these samples are heated at high temperature after being exposed to H_2O at room temperature.[13] Heinemann et al.[28] studied Li/MgO, which were prepared by different preparation methods by XPS. They found that Li/MgO samples which had a thick shoulder peak of O1s had a higher activity of the OCM reaction. Peng et al. also reported the correlation between CH_4 conversion and $[Li^+O^-]$ area of O1s.[15] From these past results, O^-(t) must be related with the OCM reaction.

Here we inquire whether this electron deficient oxide ion is really O^- or not. The most reliable data is obtained by ESR, where the anion radical can be identified like O^- on the UV-irradiated MgO for example.

We have shown that O^- on the UV-irradiated MgO could react with CH_4 at room temperature and gives surface methoxide (FT-IR). The species obtained on heat-treated MgO does not give any ESR spectra and does not react with CH_4 at room temperature, but does at 973 K. A proposed structure

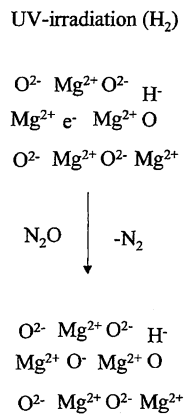

Fig. 5. The O^- generation model on the UV-irradiated MgO.

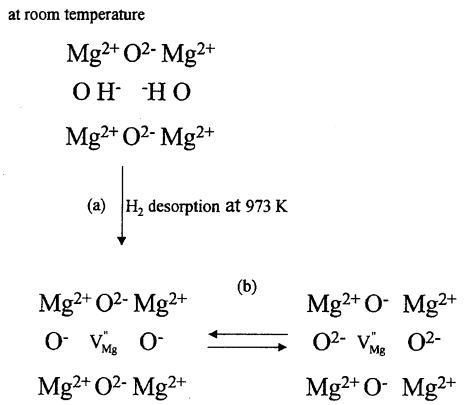

Fig. 6. The O^- generation model on the heat-treated MgO.

having O^-(u) on the UV-irradiated MgO is shown in Fig. 5. This surface is said to keep a small amount of H_2 added and to be cylindrically symmetry around O^-(u), which is analyzed and quantified by ESR.[16] The formation equation is:

$$H'_{Mg}\cdots V^{\bullet}_{O} + N_2O \rightarrow H'_{Mg}\cdots O^{\bullet}_{O} + N_2 \qquad (6)$$

The amount of O^-(u) has been estimated as about 1/10000 of that of O^{2-}, so that O^-(u) must be lonely situated on MgO. This structure is destroyed above 533 K.[29] However, much thermally generated O^-(t) was found (10%) and was not observable by ESR probably because of the spin–spin interaction owing to too much population of O^-(t). The model of O^-(t) generation by the heat-treatment is shown in Fig. 6. The two O^-(t) produced by H_2 desorption must be located across from a V''_{Mg} (Mg^{2+} defect) as shown in step (a) of Fig. 6. The two radicals may couple to decay the radical nature (no ESR) or the two mix their electrons with neighboring oxygen ions (O^{2-}) (step (b) of Fig. 6). This may be the reason why these species are not observed with the ESR method, and can not react with methane at room temperature, which is different from the nature of O^-(u) produced by the UV-irradiation.

The amount of surface oxygen anion calculated by the XPS measurements was quite high over 10%. One of the causes may be that the produced O^- is denser in the near surface than in the bulk, as the surface charge is said to be changed to positive upon calcination over 873 K.[30] In this case a part of $[O^{\bullet}_{O}V''_{Mg}O^{\bullet}_{O}]^X$ structure must be dissociated to $O^{\bullet}_{O}$ (surface) and $[V''_{Mg}O^{\bullet}_{O}]'$ (bulk) as the results of equilibrium. Therefore, the real number of O^-(t) to the total oxygen anion may not be so high as in Table 1.

Conclusions

The electron deficient oxide ion (O^-(t)) observed by XPS was found to be related with H_2 TPD and the OCM reaction. The reactivity toward CH_4 is much lower than the O^-(u) on the UV-irradiated MgO. However, the O^-(t) can react with methane at high temperature, as the oxidative coupling of methane (OCM) reaction occurs.

This work has been carried out as a research project of The Japan Petroleum Institute commissioned by Petroleum Energy Center with the support of the Ministry of International Trade and Industry.

References

1) U. Preuss and M. Baerns, *Chem. Eng. Tecnol.*, **10**, 297 (1987).
2) K. Asami, T. Shikada, K. Fujimoto, and H. Tominaga, *Ind. Eng. Chem. Res.*, **26**, 2348 (1987).
3) T. Ito and J. H. Lunsford, *Nature*, **314**, 721 (1985).
4) T. Ito, J.-X. Wang, C.-H. Lin, and J. H. Lunsford, *J. Am. Chem. Soc.*, **107**, 5062 (1985).
5) E. Iwamatsu, T. Moriyama, N. Takasaki, and K. Aika, *J. Chem. Soc., Chem. Commun.*, **1987**, 19.
6) E. Iwamatsu, T. Moriyama, N. Takasaki, and K. Aika, *J. Catal.*, **113**, 25 (1988).
7) E. C. Subbarao and H. S. Maiti, *Solid State Ionics*, **11**, 317 (1984).
8) H. Kathrein and F. Freund, *J. Phys. Chem. Solids*, **44**, 177 (1983).
9) I. Balint and K. Aika, in "Natural Gas Conversion," ed by H. E. Cury-Hyde and R. F. Howe, Elsevier, Amsterdam (1994), p. 177.
10) I. Balint and K. Aika, *J. Chem. Soc., Faraday Trans.*, **91**, 1805 (1995).
11) T. Karasuda and K. Aika, *J. Catal.*, **171**, 439 (1997).
12) E. G. Derouane and V. Indovina, *Chem. Phys. Lett.*, **14**, 455 (1972).
13) Y. Inoue and I. Yasumori, *Bull. Chem. Soc. Jpn.*, **54**, 1505 (1981).
14) T. Nishiyama and K. Aika, *J. Catal.*, **122**, 346 (1990).
15) X. D. Peng, D. A. Richards, and P. C. Stair, *J. Catal.*, **121**, 99 (1990).
16) A. Goto and K. Aika, *Bull. Chem. Soc. Jpn.*, **71**, 95 (1998).
17) C. T. Au, X.-C. Li, J.-A. Tang, and M. W. Roberts, *J. Catal.*, **106**, 538 (1987).
18) W. B. Williamson, J. H. Lunsford, and C. Naccache, *Chem. Phys. Lett.*, **9**, 33 (1971).
19) R. O. Kagel and R. G. Greenler, *J. Chem. Phys.*, **49**, 4638 (1968).
20) F. A. Kroger, "The Chemistry of Imperfect Crystals," North-Holland, Amsterdam (1964).
21) F. Freund and H. Wengeler, *J. Phys. Chem. Solids*, **43**, 129 (1982).
22) M. Che and A. J. Tench, *Adv. Catal.*, **31**, 77 (1982).
23) C. K. Jorgensen and H. Berthou, *Faraday Discuss. Chem. Soc.*, **54**, 269 (1972).
24) M. C. Wu, C. M. Truong, K. Coulter, and D. W. Goodman, *J. Am. Chem. Soc.*, **114**, 7565 (1992).
25) M. C. Wu, C. M. Truong, K. Coulter, and D. W. Goodman, *J. Vac. Sci. Technol. A*, **11**, 2174 (1993).
26) M. C. Wu, C. M. Truong, K. Coulter, and D. W. Goodman, *J. Catal.*, **140**, 344 (1993).
27) J.-L. Dubois and C. J. Cameron, *Appl. Catal.*, **67**, 49 (1990).
28) Y.-F. Chang, G. A. Somorjai, and H. Heinemann, *J. Catal.*, **141**, 713 (1993).
29) M. Iwamoto and J. H. Lunsford, *J. Phys. Chem.*, **84**, 3079 (1980).
30) M. M. Freund, F. Freund, and F. Batllo, *Phys. Rev. Lett.*, **63**, 2096 (1989).